

## Systematic calculations of the band structures of the rare-gas crystals neon, argon, krypton, and xenon

N. C. Bacalis

*Research Center of Crete, P.O. Box 527, 711 10 Heraklion, Crete, Greece*

D. A. Papaconstantopoulos and W. E. Pickett

*Condensed Matter Physics Branch, Naval Research Laboratory, Washington, D.C. 20375-5000*

(Received 26 October 1987)

Scalar relativistic self-consistent calculations of the band structure of Ne, Ar, Kr, and Xe have been performed with the augmented-plane-wave method using the Hedin-Lundqvist local-density (LD) expression for exchange and correlation. The trends with increasing atomic number in this inert-gas solid series are presented for the valence-band width, LD band gap, and for low-lying conduction-band eigenvalues. A simplified form of self-energy correction that accounts for dynamical exchange and correlation processes to the single-particle excitations is included. Comparisons are made with previous studies using different methods. The present approach is most reliable for valence-band properties and gives semiquantitative agreement with experimental values of the band-gap and conduction-band separations.

### I. INTRODUCTION

A number of studies of the electronic structure of rare-gas crystals has been presented in the past. The most systematic study of the whole class was given by Trickey *et al.*<sup>1</sup> They performed self-consistent but non-relativistic calculations using the augmented-plane-wave (APW) method in the  $X\alpha$  approximation. In this paper we present relativistic self-consistent calculations of the band structure using the APW method for the rare-gas crystals (RGC) Ne, Ar, Kr, and Xe using the exchange and correlation potential treated in the local-density theory of Hedin and Lundqvist.<sup>2</sup> A systematic comparison of the RGC, including previous related work, is made. The results have been corrected to give more realistic approximations to true excitation energies using the theory of Pickett and Wang.<sup>3</sup> A calculation of the electron momentum distribution and of Compton profiles in the impulse approximation will be given in a subsequent paper.<sup>4</sup> Also a Slater-Koster parametrization of the unoccupied states has been presented in Ref. 5. Band-structure calculations of the RGC have been performed in the past with different approximations for different elements. Rössler<sup>6</sup> has published relativistic, but non-self-consistent, calculations by the Korringa-Kohn-Rostoker (KKR) method, and Kunz and Mickish<sup>7</sup> have presented self-consistent but nonrelativistic calculations by the Hartree-Fock (HF) method. After a brief review of these and other previous calculations, we present our results and compare them with others, making a more systematic comparison with those of Rössler and Kunz and Mickish. The reason we are comparing with Rössler is that his calculations are fitted to measured values and therefore we are effectively comparing to experiment. On the other hand, the first-principles calculations of Trickey *et al.*<sup>1</sup> determined equilibrium lattice constants via total energy

calculations that are, except for Ne, very close to experiment. However, these calculations underestimate the energy gap, and when parametrized to correct the gap they underestimate the valence-band width.

### II. GENERAL REMARKS FROM RELEVANT WORKS

Individual calculations of the band structure for each of the RGC have been performed with various methods that differ mainly in the treatment of the exchange potential. This treatment is considered crucial for determining the eigenenergies, and divides the calculations into two groups; the "HF group" using the exact exchange, and the "local-density-approximation (LDA) group," using statistical exchange and including correlation in the local-density theory: [e.g.,  $\alpha=1$  (Slater),  $\alpha=\frac{2}{3}$  (Kohn-Sham, Gaspar),  $\alpha$  adjustable ( $X\alpha$ ), or Hedin-Lundqvist<sup>2</sup>]. In the HF approximation the empty virtual orbitals are generally diffuse in self-consistency, thus their energies are quite high. The lighter the nucleus the less screening appears in the electrons, the smaller the overlap of the occupied orbitals, and the narrower the valence bands; the more diffuse the virtual orbitals, the wider the conduction band.<sup>6-9</sup> Thus the HF results are characterized by wide conduction bands and large gap. Correlation corrections are necessary to reduce the gap and narrow the bands.<sup>7,9,10</sup> The LDA overestimates the correlation energy, reducing the gap to about half the experimental value and giving narrow conduction bands.<sup>6-14</sup> Although the valence bands are, with a suitable adjustment of the exchange potential, very similar to the HF bands,<sup>12</sup> this adjustment seriously affects the conduction bands. The simplest way to perform such changes is to change the  $\alpha$  parameter.<sup>8,15,16</sup> Increasing  $\alpha$  separates the bands, and the valence electrons become more tightly bound.<sup>17</sup> This improves the gap but destroys other ground-state

properties such as cohesive energy, lattice constant, and valence-band width, which otherwise are quite accurate in the LDA.<sup>11,18</sup> The valence-band width, for example, narrows with increased  $\alpha$  due to decreasing overlap.<sup>8,11,15–18</sup> Increasing the lattice constant drastically compresses the conduction band, while the gap is practically unaffected.<sup>15</sup> This effect is also due to a decrease of the overlap. It was once believed<sup>6,7</sup> that in the LDA the lighter the atom, the more compressed the conduction bands, contrary to the HF approximation and to the experiment. Generally this is not true for the LDA, where we find the correct trend. Increasing the atomic number widens the valence band, compresses the conduction band, and lowers the gap, in agreement with the HF results and the experiment,<sup>7</sup> but the magnitude of the gap is about half the experimental one. The bandwidths are quite reasonable as shown below.

Efforts have been made in the past to improve the value of the energy gap in the LDA, by either changing  $\alpha$  (Refs. 8 and 15–17) or approximating it in various ways.<sup>16,19</sup> The most promising methods seem to be the recently developed calculation of self-interaction correction<sup>14,20,21</sup> (SIC) or the single-particle excitation theory, such as that of Pickett and Wang.<sup>3</sup> We have applied the latter approach in this work and find a significant improvement in the size of the energy gap.

### III. METHOD OF CALCULATION AND APPROXIMATIONS

The RGC crystallize in the fcc structure. The lattice constants were taken from Wyckoff<sup>22</sup> and are listed in Table I. It should be noted that the lattice parameters calculated by Trickey *et al.*,<sup>1</sup> with the exception of Ne, are very close to experiment. Our calculations were performed in the muffin-tin approximation, self-consistently, on a mesh of 20  $k$  points in the  $\frac{1}{48}$  section of the first Brillouin zone (BZ), using a standard symmetrized APW code without linearization. These calculations were scalar relativistic, i.e., the Dirac equation was solved in the crystal, neglecting the spin-orbit coupling. For a general  $k$  point, 70 plane waves were used that correspond to a level of convergence better than 0.1 mRy. The crystal potential was calculated on a doubling linear mesh of 218 values inside the muffin-tin sphere. The exchange potential was calculated using the local-density theory of Hedin and Lundqvist.<sup>2</sup> For the calculation of the energy bands and the density of states, the 20- $k$ -point self-

TABLE I. Quantities used in the self-energy calculations:  $\epsilon_0$ , high-frequency dielectric constant;  $r_s$ , electron density parameter;  $E_g$ , energy gap;  $\lambda = \hbar\omega_p^0/E_F^0$ ; and  $a$ , lattice constant. The value of  $\epsilon_0$  for Ne is somewhat uncertain, due to lack of precise experimental information.

	$\epsilon_0$	$r_s$	$E_g$ (Ry)	$\lambda$	$a$ (a.u.)
Ne	(1.4)	1.80	1.53	2.27	8.3696
Ar	1.58	2.14	1.02	1.45	9.9324
Kr	1.78	2.32	0.84	1.11	10.8111
Xe	2.0	2.52	0.67	0.87	11.7106

consistent crystal potential was used to generate energies for a 33- $k$ -point mesh in the  $\frac{1}{48}$  of the first BZ. Then the energy bands were calculated on a fine  $k$ -point mesh by a Fourier-series interpolation taking into account the compatibility relations.<sup>23</sup> These interpolated bands were used to calculate the density of states by the tetrahedron method.<sup>24</sup> The core levels were treated in the soft-core approximation as described elsewhere.<sup>25</sup> The above choices are considered as the optimum ones for accurate results and reasonable computing time, according to the results of a study of various approximations in APW calculations.<sup>25</sup> The APW results were corrected using the self-energy function of the single-particle excitation<sup>3</sup> as described in the next section.

### IV. SELF-ENERGY CALCULATION

It is now well understood that the LDA underestimates the energy gap of nonmetals. Formally there is no justification for interpreting the LDA gap as the optical gap, but Pickett and Wang<sup>3</sup> and others have shown that an appropriately defined self-energy can be added to the LDA bands to give true excitation energies. Their formulation leads to very good energy gaps in a variety of semiconductors<sup>3</sup> (Si, GaP, SiC, diamond). For Ge and GaAs the resulting gaps are poor, but this appears to be due to the extremely small gaps given by LDA in these materials; the self-energy should be applied (ideally) to the exact density-functional gap, which is unknown.

This self-energy correction, which has not previously been applied to wide-gap insulators, is included here for the rare-gas solids as a first test for this class of materials. The self-energy is based on the “ $GW$  approximation” of Hedin<sup>26</sup> and others,<sup>3</sup> where  $G$  denotes the single-particle Green’s function and  $W$  is the dynamically screened Coulomb interaction

$$W(k, \omega) = \frac{v(k)}{\epsilon(k, \omega)} = \frac{4\pi e^2}{\Omega k^2 \epsilon(k, \omega)}, \quad (1)$$

where  $\Omega$  is the normalization volume. The  $GW$  approximation has been studied most thoroughly for the electron-gas problem, where the random-phase approximation (RPA) is a reasonable choice for dielectric function  $\epsilon(k, \omega)$ .

The application of this approach to crystalline nonmetals required two essential generalizations: (1) the underlying spectrum in  $G$  was generalized to include a gap  $E_g$ , and (2) the RPA dielectric function must be made appropriate for a nonmetal, which differs from that of a metal in both its  $k$  and  $\omega$  dependence. This was done using the screening function of Levine and Louie,<sup>20</sup> which introduces a single constant  $\lambda$  but produces a realistic and causal screening behavior. This constant is determined by the static, long-wavelength dielectric constant  $\epsilon_0$  through the defining equation

$$\lambda E_F^0 = \hbar\omega_p^0 / (\epsilon_0 - 1)^{1/2}, \quad (2)$$

where  $E_F^0$  and  $\omega_p^0$  are the Fermi energy and plasma frequency of the electron gas with density equal to the aver-

age valence electron density of the solid. Since  $\epsilon_0$  and  $E_g$  can be calculated from the resulting corrected band structure,  $\lambda$  and  $E_g$  can be determined self-consistently, but this has not been necessary in the previous studies and will not be attempted here. The various parameters entering the calculations for the RGC are given in Table I.  $E_G$  was chosen from a zone average of the direct band gap, anticipating the self-energy correction which would result and including it in accordance with Eq. (3) for  $\tilde{E}_k$ .  $E_G$  is thus very close to the zone average of the direct gap in the *quasiparticle* bands, that is, it is self-consistent.

The Pickett-Wang theory leads to a self-energy correction which enters as an energy- and density-dependent potential. (As in the previous studies the imaginary part will be neglected, as it vanishes for bands near the gap.) Since we are primarily interested in determining the magnitude of the correction, we make the simplifying approximation of evaluating the density variable in the self-energy always at the average valence electron density. This "mean-density approximation" was shown to give most of the correction in the previous studies.

The correction then is given by

$$\tilde{E}_k = E_k^{\text{LDA}} + \bar{\Sigma}(\tilde{E}_k), \quad (3)$$

a simple scalar equation for the excitation energy  $\tilde{E}_k$  in terms of the LDA eigenvalue  $E_k^{\text{LDA}}$  which converges easily by iteration once the "mean-density self-energy"  $\bar{\Sigma}(E)$  is determined. Before discussing the results, it is worthwhile to recall the basis of the Pickett-Wang theory. The self-energy was formulated in terms of a homogeneous semiconducting electron-gas model which should be a good ansatz when the gap is small compared to the valence-band width, which has been true in the previous studies.<sup>3</sup> This ratio of gap to valence-band width is reflected in the constant  $\lambda$ , which is of the order of 0.25–0.5 for semiconductors. From Table I it can be seen that  $\lambda$  for the rare-gas solids lies above the range of formal validity of the theory. These values of  $\lambda$  range from 0.87 to 2.27 and reflect the large gaps and small valence-band widths in these insulators. In addition, in making our mean-density approximation, we are neglecting a systematic difference between the valence and conduction states, which is that the valence  $p$  states are strongly bound near the atoms and lie in a higher than average density region, while the conduction states lie much more in the interstitial region and therefore sample a lower electron density. As a result the mean-density approximation may tend to lead to smaller corrections than the full theory would give.

## V. RESULTS AND COMPARISONS

We consider first the APW results in the LDA before applying the self-energy correction. In Fig. 1 we have plotted as a function of  $Z$  certain characteristic levels which reflect the variation of the energy gap and the width of the conduction band. We have taken as the origin the state  $\Gamma_{15}$  which is the top of the valence band which we have also indicated as the Fermi level in our figures of the energy bands. We note from Fig. 1(a) that the value of the conduction  $\Gamma_1$  level decreases as a function of  $Z$  from 0.838 Ry for Ne to 0.409 Ry for Xe. These widths represent the energy gap between valence and conduction bands and, as expected in the LDA, are much smaller than the measured values. The positions of the  $d$ -like levels  $\Gamma_{25'}$  and  $\Gamma_{12}$  with respect to the  $s$ -like  $\Gamma_1$  level describe the  $s$ - $d$  separation and the  $d$ -band width of the conduction bands. We note that similarly to the energy gap the  $s$ - $d$  separation decreases as a function of  $Z$  while the  $d$ -band width undergoes a decrease by more than a factor of 2 from Ne to Ar and then remains approximately constant for Kr and Xe. Although they overestimate the measured values as analyzed by Rössler,<sup>6</sup> these conduction-band widths are in closer agreement to experiment than the energy gap.

Applying the self-energy correction causes a substantial increase in the value of the energy gap which brings our results to approximately 10% under the measured values. On the other hand, the self-energy correction gives a moderate increase of the conduction-band separations which worsens the agreement with experiment. Figure 1(b) shows the variation with  $Z$  of the levels  $\Gamma_1$ ,  $\Gamma_{25'}$ , and  $\Gamma_{12}$  for our self-energy corrected results.

Tables II, III, IV, and V show a detailed comparison at

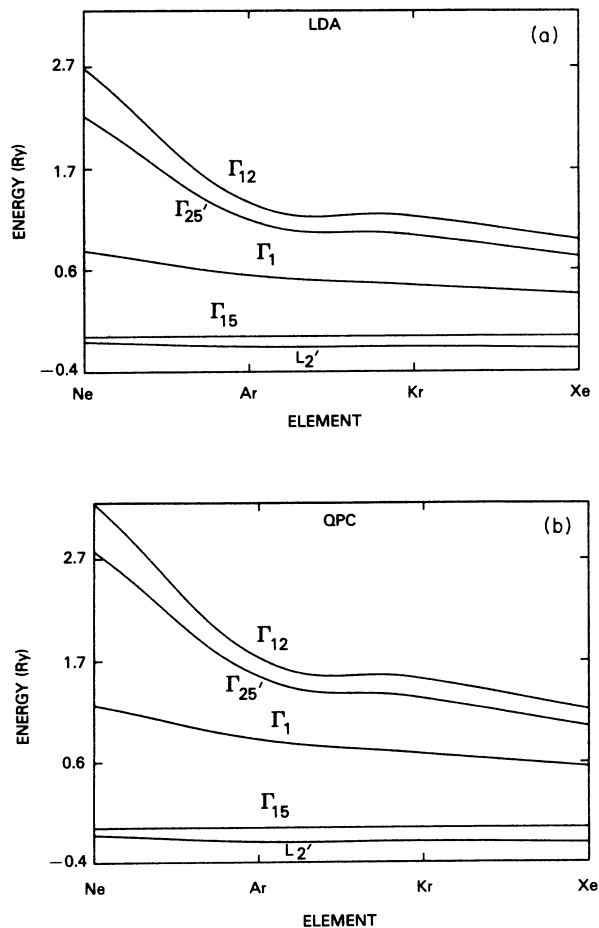


FIG. 1. Characteristic widths as a function of element.

TABLE II. Energies at high-symmetry points for solid neon.

		This work		Ref. 9	Ref. 7	Ref. 6	Expt.	
		LDA	QPC					
Gap	$\Gamma_1$	0.838	1.217	1.868	1.629	1.526	1.526 <sup>a</sup>	
	$\Gamma_{12}$	2.635	3.192					
	$\Gamma_{15}$	2.498	3.056	3.494	3.890			
	$\Gamma_{25'}$	2.170	2.724	3.201		2.702		
	$\Gamma_{2'}$	2.314	2.872	3.278				
	$X_1$		1.339	1.813	2.348	2.618	2.040	
			2.298	2.856	3.362			
	$X_2$	3.062	3.621					
	$X_3$	1.677	2.193	2.693		2.335		
	$X_5$	3.163	3.723					
	$X_{4'}$	1.399	1.881	2.420	2.235	2.07		
	$X_{5'}$	1.949	2.489	2.972	2.926	2.62		
	$L_1$		1.281	1.746	2.315	2.201	1.96	
			2.067	2.615	3.084		2.70	
			1.249	1.709	2.254	2.063	1.85	
			2.208	2.765	3.169			
			2.419	2.977	3.477	3.566		
	$\Gamma_{15}$		0.000	0.000	0.000	0.000	0.000	
		$X_{4'}$	-0.049	-0.065	-0.034	-0.022		
$X_{5'}$		-0.017	-0.022	-0.012	-0.000			
VBW	$L_{2'}$	-0.055	-0.073	-0.036	-0.029		-0.096 <sup>b</sup>	
	$L_{3'}$	-0.005	-0.007	-0.019	0.000			
	$W_{2'}$	-0.018	-0.024					
	$W_3$	-0.033	-0.044					
CBW	$\Gamma_{25'}-\Gamma_1$	1.332	1.508			1.176		
	$X_1-\Gamma_1$	0.501	0.597		0.989	0.514		
	$L_1-\Gamma_1$	0.443	0.530		0.571	0.440		

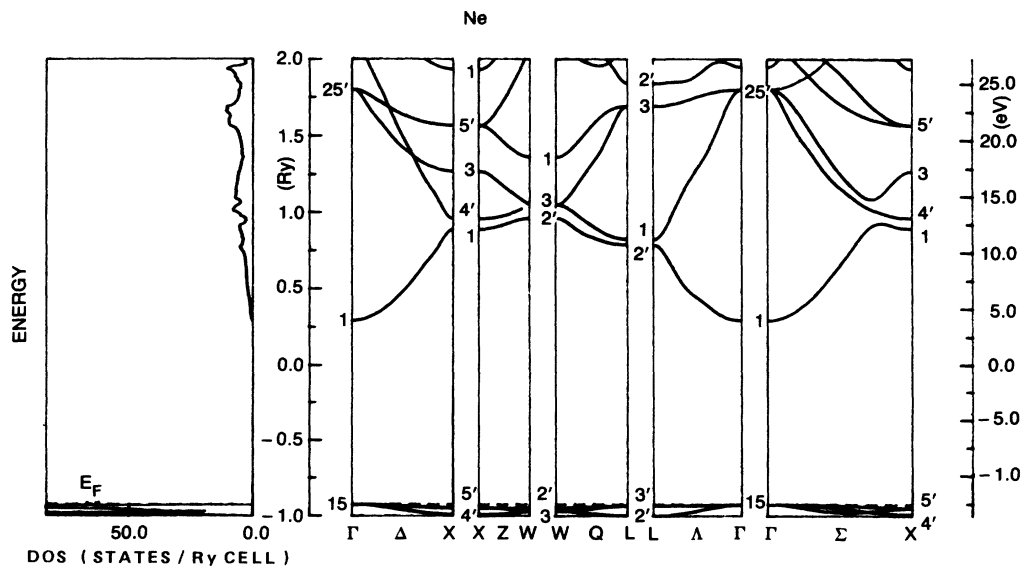
<sup>a</sup>Reference 6.<sup>b</sup>Reference 27.

FIG. 2. The band structure and density of states for solid neon.

TABLE III. Energies at high-symmetry points for solid argon.

		This work		Ref. 13	Ref. 9	Ref. 7	Ref. 6	Ref. 16	Expt.
		LDA	QPC						
Gap	$\Gamma_1$	0.595	0.879	0.979	1.361	1.119	1.015	0.955	1.015 <sup>a</sup>
	$\Gamma_{12}$	1.313	1.682	1.518	2.194	2.066	1.51	1.472	
	$\Gamma_{15}$	1.699	2.079	2.692	2.456	3.397			
	$\Gamma_{25'}$	1.141	1.499	1.411	1.972	1.860	1.397	1.359	
		2.325	2.701			3.316			
	$\Gamma_{2'}$	1.494	1.869		2.245				
	$X_1$	0.788	1.107	1.168	1.551	1.340	1.188	1.138	
		1.657	2.038	1.856	2.525	3.272			
	$X_2$	1.437	1.812	1.592		2.184	1.640	1.555	
	$X_3$	0.909	1.245	1.251	1.865	1.536	1.221	1.201	
		2.080	2.456			3.037			
	$X_5$	1.476	1.852	1.620		2.221	1.60	1.582	
	$X_{4'}$	1.099	1.454	1.410	1.865	1.691	1.51	1.395	
	$X_{5'}$	1.444	1.818	1.783	2.227	2.250	1.64		
	$L_1$	0.813	1.136	1.176	1.593	1.396	1.136	1.133	
		1.575	1.955	1.756	2.472	2.419			
	$L_3$	1.110	1.466	1.397	1.927	1.838	1.37	1.347	
		1.436	1.811	1.598	2.357	2.184	1.62	1.557	
	$L_{2'}$	0.971	1.314	1.297	1.712	1.550	1.37	1.298	
		1.449	1.823		2.197	1.44			
	$L_{3'}$	1.762	2.142	2.770	2.560	2.963			
	$\Gamma_{15}$	0.000	0.000	0.000	0.000	0.000		0.000	
	$X_{4'}$	-0.094	-0.127	-0.041	-0.084	-0.074		-0.047	
	$X_{5'}$	-0.034	-0.046	-0.015	-0.033	-0.007		-0.018	
VBW	$L_{2'}$	-0.104	-0.141	-0.044	-0.009	-0.088		-0.051	-0.125 <sup>b</sup>
	$L_{3'}$	-0.012	-0.015	-0.005	-0.013	-0.088		-0.006	
	$W_{2'}$	-0.066	-0.051	-0.016				-0.019	
	$W_3$	-0.038	-0.089	-0.028				-0.033	
CBW	$\Gamma_{25'}-\Gamma_1$	0.546	0.621			0.741	0.313		0.382
	$X_1-\Gamma_1$	0.193	0.228			0.221	0.180		0.173
	$L_1-\Gamma_1$	0.216	0.257			0.277	0.125		0.121

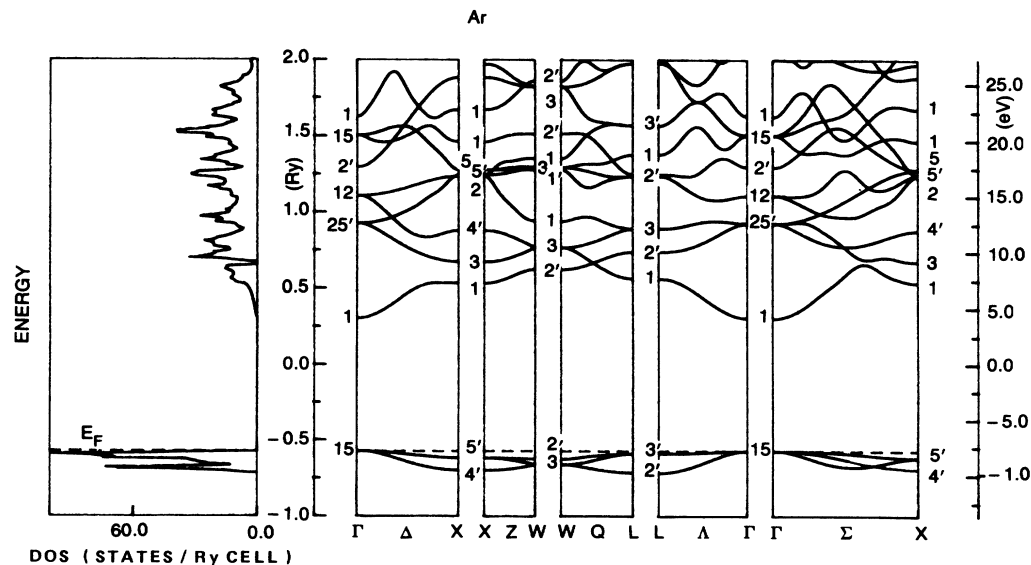
<sup>a</sup>Reference 6.<sup>b</sup>Reference 27.

FIG. 3. The band structure and density of states for solid argon.

high symmetry points of our LDA and our quasiparticle (QP) corrected results to those from other studies. The origin of the energy scale is shifted to the top of the valence band  $\Gamma_{15}$ . Other results are given for completeness, but a comparison is made mainly with the experiment adjusted bands of Rössler,<sup>6</sup> and the correlation corrected results of Kunz and Mickish (KM).<sup>7</sup> The experimental values for the valence-band widths and gaps are taken from Schwentner *et al.*<sup>27</sup> and from Rössler.<sup>6</sup> The experimental gaps and bandwidths are given in the last column of Tables II–V. Figures 2–5 show the energy bands and densities of states including the QP correction.

### A. Neon

Table II shows typical energy levels from various calculations and experiments and Fig. 2 shows the energy bands and total density of states (DOS). As we mentioned above, the LDA band gap is just over half the ex-

perimental value, while our self-energy correction brings it to within 20% under the measured value. The results of KM overestimate the gap by 10%. For the valence-band width (VBW) our LDA results are much better than for previous studies. We find a width of 0.055 Ry while KM find 0.029 Ry compared to the experimental value of 0.096 Ry. Our QP corrected results give a VBW of 0.073 Ry in even better agreement with experiment. For the conduction band we have tabulated the energy differences  $\Gamma_{25'}-\Gamma_1$ ,  $X_1-\Gamma_1$ , and  $L_1-\Gamma_1$  to provide a measure of the bandwidths. We note that our LDA results are in close agreement with the experiment adjusted values of Rössler. Our QP corrected results overestimate the measured values by about 20% while those of KM exceed the experimental values even more. The energy bands of Fig. 2 are wide and free-electron-like.

### B. Argon

Our results for Ar are shown in Fig. 3 and Table III. The energy bands are narrower than those of Ne with the

TABLE IV. Energies at high-symmetry points for solid krypton.

		This work		Ref. 29	Ref. 10	Ref. 7	Ref. 6	Expt.
		LDA	QPC					
Gap	$\Gamma_1$	0.497	0.734	0.84	1.112	0.998	0.838	0.838 <sup>a</sup>
	$\Gamma_{12}$	1.171	1.468	1.50	1.875	1.772 4.051	1.32	
	$\Gamma_{15}$	1.416	1.714	1.80	2.071	3.103		
	$\Gamma_{25'}$	0.986 2.264	1.279 2.551	1.36	1.728	1.581 3.618	1.220	
	$X_1$	0.659 1.434	0.926 1.729	1.04 1.85	1.261 2.212	1.175 2.382	1.000	
	$X_2$	1.322	1.619	1.65	2.088	1.912	1.47	
	$X_3$	0.766 1.994	1.044 2.281	1.10	1.382	1.306 3.301	1.04	
	$X_5$	1.371	1.667	1.76	2.378	1.956	1.43	
	$X_{4'}$	0.982	1.274	1.42	1.656	1.581	1.34	
	$X_{5'}$	1.251	1.548	1.74	1.934	2.059	1.47	
	$L_1$	0.680 1.409	0.950 1.705	1.026 1.895	1.303 2.170	1.237 2.154	0.948	
	$L_3$	0.955 1.317	1.245 1.615	1.375 1.805	1.522 1.857	1.544 1.912	1.19 1.44	
	$L_{2'}$	0.865 1.210	1.151 1.507	1.355	1.509 1.849	1.435	1.19 1.25	
	$L_{3'}$	1.493	1.787	1.895	2.186	3.551		
	$\Gamma_{15}$	0.000	0.000	0.000	0.000	0.000		
	$X_{4'}$	−0.095	−0.125	−0.085	−0.190	−0.088		
	$X_{5'}$	−0.035	−0.047	−0.035	−0.035	−0.015		
VBW	$L_{2'}$	−0.105	−0.138	−0.095	−0.208	−0.103		−0.169 <sup>b</sup>
	$L_{3'}$	−0.012	−0.016	−0.015	−0.029	−0.000		
	$W_{2'}$	−0.039	−0.052					
	$W_3$	−0.067	−0.089					
CBW	$\Gamma_{25'}-\Gamma_1$	0.489	0.541			0.583	0.360	0.382
	$X_1-\Gamma_1$	0.162	0.189			0.177	0.180	0.162
	$L_1-\Gamma_1$	0.183	0.212			0.239	0.132	0.110

<sup>a</sup>Reference 6.

<sup>b</sup>Reference 27.

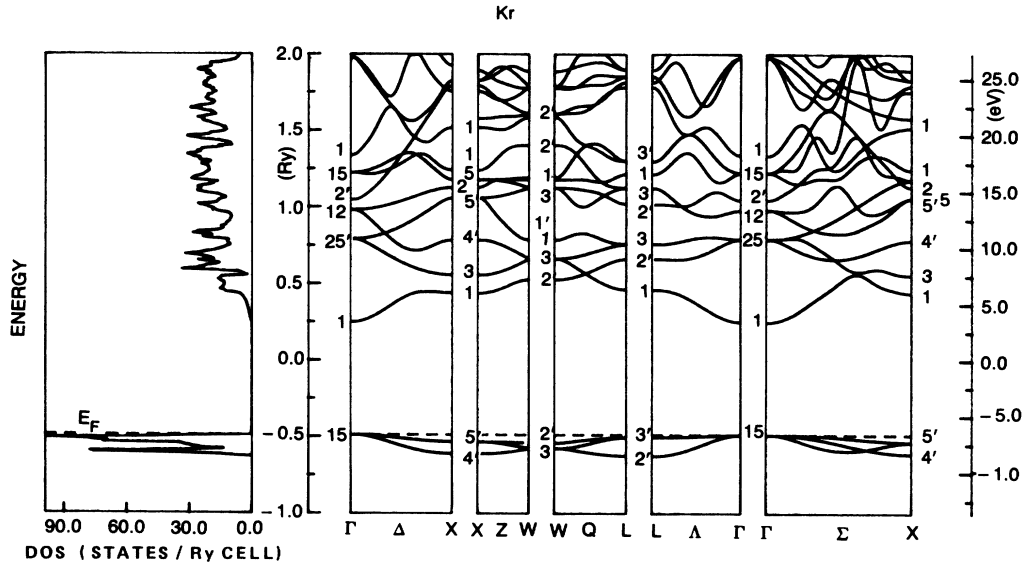


FIG. 4. The band structure and density of states for solid krypton.

conduction bands looking similar to the  $s$ - $d$  complex of bands in a transition metal. The LDA band gap is 60% of the experimental value while the self-energy correction improves our result to almost 90%. KM, including correlation corrections, overestimate the gap by about 10%. As in Ne the VBW is in much better agreement with experiment than both previous LDA calculations and the Hartree-Fock calculations of KM. We find a width of 0.104 Ry while KM, Mattheiss,<sup>13</sup> and Azama,<sup>16</sup> find 0.096, 0.044, and 0.051 Ry, respectively, the experimental value being 0.125 Ry. Trickey *et al.*<sup>11</sup> found a VBW of 0.121 Ry in excellent agreement with experiment, but with the usual underestimation of the gap. They parametrized the exchange coefficient  $\alpha$  to correct the value of the gap, but this resulted in a VBW of 0.050 Ry. Our QP correction (QPC), while it gives an excellent value for the gap, retains the good agreement of the VBW with experiment.

The conduction-band separations from  $\Gamma_1$  are also shown in Table III. Both our LDA and QPC values are between those of KM and experiment.

### C. Krypton

Krypton has also been studied extensively, and similar conclusions to those of Ar can be drawn from Table IV and Fig. 4. We find a LDA gap of 0.497 Ry, increasing to 0.734 Ry after we applied the self-energy correction while the experimental value is 0.838 Ry, and that of KM is 0.998 Ry. The VBW is found to be 0.105 Ry from the LDA and 0.138 Ry from the QPC which is close to the experimental value of 0.169 Ry. The VBW's given by KM and Trickey *et al.*<sup>11</sup> are 0.103 and 0.116 Ry, respectively.

The conduction-band separations from  $\Gamma_1$  are also shown in Table IV. Our results are again between those of KM and experiment but closer to experimental values than in Ne and Ar. Again all calculations overestimate

TABLE V. Energies at high-symmetry points for solid xenon.

		This work		Ref. 6	Expt.
		LDA	QPC		
Gap	$\Gamma_1$	0.409	0.605	0.673	0.673 <sup>a</sup>
	$\Gamma_{12}$	0.944	1.172	1.07	
	$\Gamma_{25'}$	0.777	1.004	0.945	
	$X_1$	0.508	0.718	0.820	
	$X_2$	1.088	1.313	1.21	
	$X_3$	0.587	0.805	0.82	
	$X_5$	1.136	1.360	1.20	
	$X_{4'}$	0.884	1.113	1.13	
	$X_{5'}$	1.056	1.281	1.22	
	$L_1$	0.539	0.752	0.791	
	$L_3$	0.751	0.977	0.95	
		1.083	1.309	1.18	
	$L_{2'}$	0.765	0.992	0.96	
		0.963	1.191	1.05	
	$L_{3'}$	1.189	1.412		
VBW	$\Gamma_{15}$	0.000	0.000		
	$X_{4'}$	-0.112	-0.140		
	$X_{5'}$	-0.043	-0.056		
	$L_{2'}$	-0.123	-0.153		-0.221 <sup>b</sup>
	$L_{3'}$	-0.015	-0.019		
CBW	$W_{2'}$	-0.049	-0.063		
	$W_3$	-0.081	-0.103		
	$\Gamma_{25'}-\Gamma_1$	0.368	0.399	0.276	0.272
	$X_1-\Gamma_1$	0.099	0.113	0.103	0.147
	$L_1-\Gamma_1$	0.130	0.147	0.099	0.118

<sup>a</sup>Reference 6.<sup>b</sup>Reference 27.

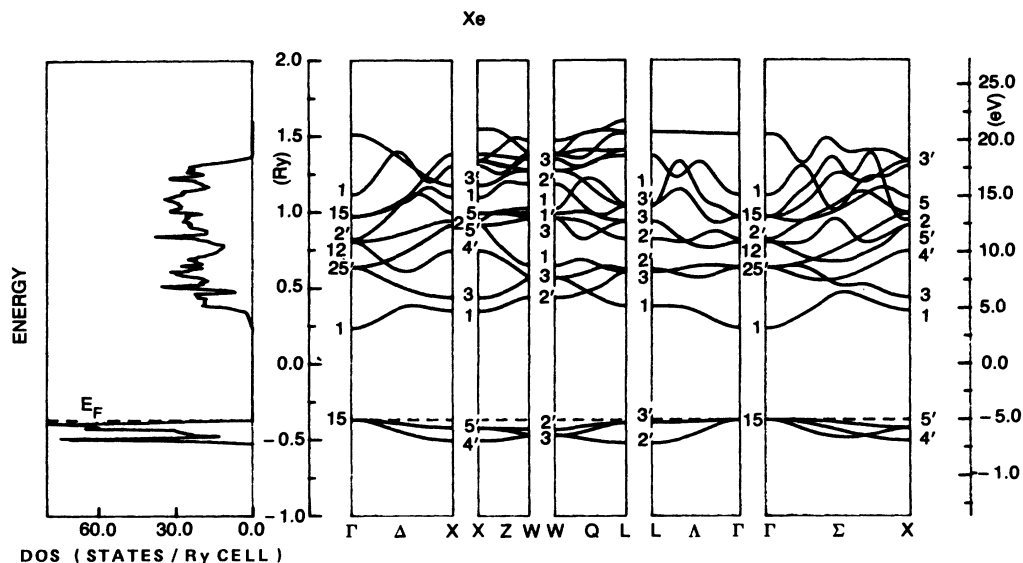


FIG. 5. The band structure and density of states for solid xenon.

the conduction-band separations compared to experiment.

#### D. Xenon

In xenon relativistic effects should be rather important. Our calculations do not include the spin-orbit (SO) coupling while they were included in the semiempirical calculations of Rössler. As a result the comparisons shown in Table V are not accurate for the  $k$  points that split due to the SO interaction. Our LDA band gap is 0.409 Ry and our self-energy corrected result is 0.605 Ry compared to the experimental value of 0.673 Ry. The VBW increases from a LDA value of 0.123 Ry to the QP corrected value of 0.153 while experiment gives 0.221 Ry. Trickey *et al.*<sup>12</sup> give an energy gap of 0.452 Ry and a VBW of 0.133 Ry. Studies of the band gap as a function of pressure are given in Ref. 28.

The conduction-band separations are also shown in Table V. As in the other inert solids our results overestimate the measured values. Figure 5 shows the energy bands and DOS for Xe. These bands (within the approximation of neglecting the SO interaction) are similar to those of Kr. Both Kr and Xe have energy bands much narrower than the other two inert solids.

## VI. CONCLUSIONS

From the figures and the tables we see that the main features of the band structures of the RGC are that in go-

ing from Ne to Xe (i) the valence-band width increases, (ii) the conduction-band separations decrease, and (iii) the energy gap decreases. These three features have also been seen experimentally. While the Hartree-Fock calculations find the same trends, that is not the case with all previous LDA calculations.<sup>6</sup> Apart from these trends quantitative comparisons show that (i) the calculated valence bands are, in all approximations, more compressed than the experiment shows, (ii) the calculated conduction bands are all wider than experiments indicate, and (iii) the band gaps are narrower in the LD, and wider in the HF, approximation. However, both the LD and the HF results come close to the measured band gaps when the self-energy and correlation corrections are applied to the respective methods. In addition, the relativistic APW calculation with HL correlation and exchange potential (this work) gives better valence-band widths and conduction-band separations than the HF (Ref. 7) and the KKR (Ref. 6) results. Evidently the ground-state properties are the most reliable, the conduction bands are less accurate, and the gaps are reasonable when the self-energy correction is applied. Our results are used in two applications, both of which are not sensitive to the value of the energy gap. One application is for the Slater-Koster parametrization<sup>5</sup> of the conduction bands of the inert-gas solids for general use, and the second is for the calculation of the electron momentum distributions and the Compton profiles presented in a subsequent paper.<sup>4</sup>

<sup>1</sup>S. B. Trickey, F. R. Green, Jr., and F. W. Averill, *Phys. Rev. B* **8**, 4822 (1973).

<sup>2</sup>L. Hedin and B. I. Lundqvist, *J. Phys. C* **4**, 2064 (1971).

<sup>3</sup>W. E. Pickett and C. S. Wang, *Phys. Rev. B* **30**, 4719 (1984); *Int. J. Quant. Chem. Symp.* **20**, 299 (1986).

<sup>4</sup>N. I. Papanicolaou and N. C. Bacalis (unpublished).

<sup>5</sup>D. A. Papaconstantopoulos, *Handbook to the Band Structure of Elemental Solids* (Plenum, New York, 1986).

<sup>6</sup>U. Rössler, *Physica Status Solidi B* **42**, 345 (1970); U. Rössler, in *Rare-Gas Solids*, edited by M. L. Klein and J. A. Venables



- (Academic, New York, 1975), p. 545.
- <sup>7</sup>A. B. Kunz and D. J. Mickish, *Phys. Rev. B* **8**, 779 (1973).
- <sup>8</sup>M. A. Khan and J. Callaway, *Phys. Lett.* **76A**, 441 (1980).
- <sup>9</sup>L. Dagens and F. Perrot, *Phys. Rev. B* **5**, 641 (1972).
- <sup>10</sup>N. O. Lipari, *Physica Status Solidi B* **40**, 691 (1970).
- <sup>11</sup>S. B. Trickey, A. K. Ray, and J. P. Worth, *Physica Status Solidi B* **106**, 613 (1981).
- <sup>12</sup>J. W. D. Connolly, in *Modern Theoretical Chemistry*, edited by G. Segal (Plenum, New York, 1976), Vol. 7, p. 105.
- <sup>13</sup>L. F. Mattheiss, *Phys. Rev.* **133**, A1399 (1964).
- <sup>14</sup>M. R. Norman and J. P. Perdew, *Phys. Rev. B* **28**, 2135 (1983).
- <sup>15</sup>A. K. Ray and S. B. Trickey, *Phys. Rev. B* **24**, 1751 (1981); **28**, 7352 (1983).
- <sup>16</sup>M. Azuma, *J. Phys. Soc. Japan* **49**, 2141 (1980).
- <sup>17</sup>J. P. Worth, C. Lee Merry, and S. B. Trickey, *J. Phys. Chem. Solids* **41**, 623 (1980).
- <sup>18</sup>S. B. Trickey and J. P. Worth, *Int. J. Quantum Chem., Quantum Chem. Symp.* **11**, 529 (1977).
- <sup>19</sup>G. Petrillo, *Nuovo Cimento* **6D**, 142 (1985).
- <sup>20</sup>R. A. Heaton, J. G. Harrison, and C. C. Lin, *Phys. Rev. B* **28**, 5992 (1983).
- <sup>21</sup>Z. H. Levine and S. G. Louie, *Phys. Rev. B* **25**, 6310 (1982).
- <sup>22</sup>R. W. G. Wyckoff, *Crystal Structures* (Interscience, New York, 1963).
- <sup>23</sup>L. L. Boyer, *Phys. Rev. B* **19**, 2824 (1979).
- <sup>24</sup>G. Lehmann and M. Taut, *Physica Status Solidi B* **54**, 469 (1972).
- <sup>25</sup>N. C. Bacalis, K. Blathras, P. Thomaides, and D. A. Papaconstantopoulos, *Phys. Rev. B* **32**, 4849 (1985).
- <sup>26</sup>L. Hedin, *Phys. Rev.* **139**, A796 (1965).
- <sup>27</sup>N. Schwentner, F.-J. Himpsel, V. Savle, M. Skibowski, W. Steinmann, and E. E. Koch, *Phys. Rev. Lett.* **34**, 528 (1975).
- <sup>28</sup>J. P. Worth and S. B. Trickey, *Phys. Rev. B* **19**, 3310 (1979); M. Ross and A. K. McMahan, *ibid.* **21**, 1658 (1980).
- <sup>29</sup>W. B. Fowler, *Phys. Rev.* **132**, 1591 (1963).